

The Geometrical Properties of Human Femur and Tibia and Their Importance for the Mechanical Behaviour of These Bone Structures*

M. Martens², R. Van Audekercke¹, P. De Meester¹, and J. C. Mulier²

¹ICOB, Biomechanics and Biomaterials Section, K. U. Leuven, Belgium

²Academisch Ziekenhuis, B-3041 Pellenberg, Belgium

Summary. A series of non pathological human tibial and femoral bones have been tested in torsional loading at high strain rates.

Elastic (torsional stiffness) and ultimate properties (T_{\max}) have been determined. A geometrical description of the individual bone structures has been performed by determination of the polar moment of inertia (assuming axial symmetry), variation of this parameter along the long axis of the bone and length of the specimen between the grips.

A fairly accurate prediction of mechanical behaviour of bone structures could be obtained using these geometrical parameters.

The high variation of elastic and ultimate properties of whole bone structures in torsional loading is primarily the result of the high variation of polar moment of inertia for the different bone specimens.

Introduction

Important experimental work has been conducted in the last two decades on the material properties of human cortical bone (Currey 1970; Evans 1973). However studies on the mechanical behaviour of whole bone structures are scarce. The strength of whole bone has been tested in bending by Knese et al. (1956), Motoshima (1960), Mather (1968) and Ehler (1970).

Azang (1972) tested tibial bones in bending and torsion and noticed a relationship between fracture

moment and frontal diameter of the proximal tibial epiphysis for bending and torsional loading.

Frankel and Burstein (1965) conducted torsional loading tests on preserved tibiae determining thereby the weakening of a bone structure after removal of a cortical bone graft due to the open section effect.

Viano et al. (1976) determined young's modulus (E), density (ρ) and shear modulus (G) of compact cortical bone by a non invasive approach on whole bone structures (female femurs) measuring resonance frequencies and associated mode shapes for bending, axial and torsional vibration modes. Geometrical features as compact area, moments of inertia and radii of gyration at different cross sections of the femurs were used for the calculation of resonance frequencies, mode shapes and material properties. Geometrical properties of human tibiae have been studied by Minns (1975) et al. by determining the second moments of area about the antero-posterior and medio-lateral planes of four human tibiae.

The most accurate method to establish a relationship between geometry and mechanical behaviour of a bone structure would be a two or three dimensional finite element analysis. Only a few studies deal (Orne et al. 1976) with the approach and many assumptions were still introduced. Since the shape of a bone varies considerably from one individual to another the whole intricate and time consuming procedure would have to be repeated for every individual bone and a description of the geometry of a bone, accurate enough to serve the cause of a finite element analysis, can hardly be obtained from an in vivo situation.

This study analyses the mechanical characteristics of the human tibia and femur in torsional loading with

* Supported by grant nr. 300071.76—Fonds voor Geneeskundig Wetenschappelijk Onderzoek

Offprint requests to: M. Martens, M.D. (address see above)

special reference to material and geometrical properties of the individual bones.

Material and Methods

This study is concerned with femoral and tibial bones from forty-two autopsy subjects ranging in age from 27 to 92 years of age. Fresh human tibial and femoral bones were dissected, labeled and stored in a freezer at -20°C before testing. Careful screening of the bone samples was performed by taking A.P. and lateral radiographical films of the bones, studying medical records and sending questionnaires to the family and family doctor of the deceased. As a result of this check several bones have been discarded from the group because of local alterations in the bone (old fracture, metastasis, Paget disease) or pathophysiological osteoporosis (steroids medication, hemiplegia, bedridden for a long period).

Through a cooperative program with the Biomechanics Laboratory of Case Western University, Cleveland, Ohio, one bone has been tested on its material properties while the mate for several pairs of bone was used to determine the mechanical behaviour of a whole bone structure in torsional loading. The mechanical tests were performed on wet specimens at high strain rates.

The method of sample preparation and torsion tests for material specimens (Burstein 1972; Reilly 1974) and for whole bone structures (Burstein 1971; Martens 1980) have been described previously. The geometrical properties of the bone specimens have been determined as follows.

Using a Cameron Bone Mineral Analyzer (Cameron 1968) bone mass and width of the cross section were determined at 2 cm intervals along the length of the bone sample (Fig. 1) which is kept in wet condition during this procedure. The polar moment of inertia, assuming a hollow cylinder with circular cross-section can be computed from these data by the equation

$$I_p = \frac{M}{4\rho_m} \left(d - \frac{2M}{\pi\rho_m} \right)$$

I_p = polar moment of inertia

M = mineral mass per unit length

d = diameter of the cross section

ρ_m = mineral content per cubic centimeter (obtained from a scanning of cortical bone samples with known dimensions).

These values of I_p , taken at 2 cm intervals, are plotted versus the position along the long axis of the bone (Figs. 8 and 9).

Elastic Behaviour

Torsional stiffness (S) of a structure can be defined as the ratio of applied torque to resultant angular deformation in the elastic region of the load deformation curve. The slope of the elastic portion of the curve represents the structural stiffness in torsion. This value has been determined for tibial and femoral bone specimens. This elastic parameter for structures has also been estimated based upon information of minimum polar moment of inertia along the long axis of the bone specimens, length of the specimens, and for a particular group also the material property (shear modulus G) was taken into account. In model one the bone is supposed to behave as an uniform hollow cylinder with a polar moment of inertia equal to the minimum I_p determined for each bone specimen (Fig. 2).

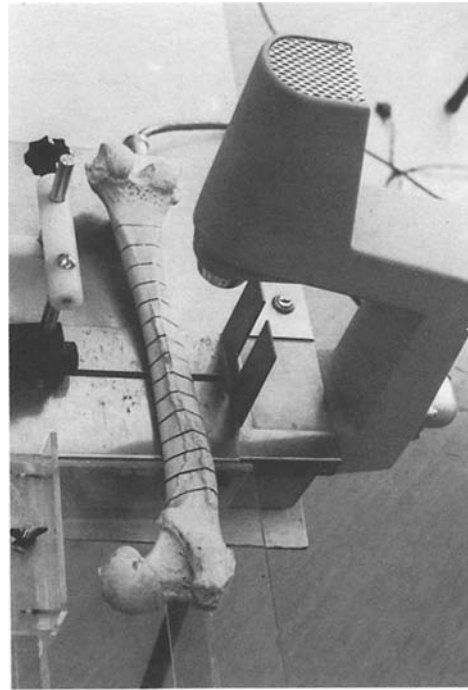


Fig. 1. Bone mass and width of the cross section are determined at 2 cm intervals using a Cameron Bone Mineral Analyzer

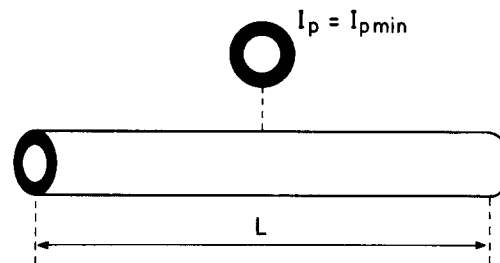


Fig. 2. For estimation of elastic and ultimate properties of femoral and tibial bone structures the bone geometry in model is an uniform hollow cylinder with I_p equal to I_{pmin} for each bone specimen and a length equal to the distance between the epoxy imbedding for a given specimen

The calculated stiffness (S_1) is given by the equation:

$$S_1 = \frac{G_m \cdot I_{pmin}}{L} \quad (1)$$

where G_m = shear modulus = $3.28 \times 10^9 \text{ N/m}^2$.

This value is the mean of the values measured by Reilly et al. (1975) in a torsion test for 166 prismatic cortical bone specimens.

I_{pmin} = minimum polar moment of inertia, calculated from the measurements with the Cameron Bone Mineral Analyser.

L = length between the imbedding in the epoxy blocks of the specimen.

Estimated and actual value of torsional stiffness for tibial and femoral bone specimens are correlated (Fig. 3).

For a particular group with known shear modulus (G) this material property was taken into account using the equation:

$$S'_1 = \frac{G_i \cdot I_{pmin}}{L}$$

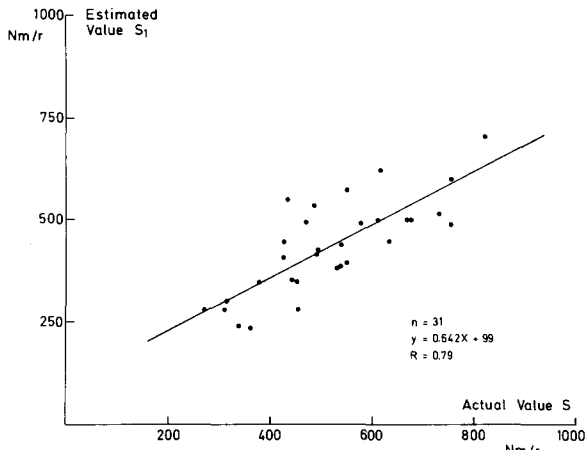


Fig. 3 a, b. Scatter plot of actual value of torsional stiffness (S) versus estimated value (S_1) based upon model one. **a** Femoral bone specimens

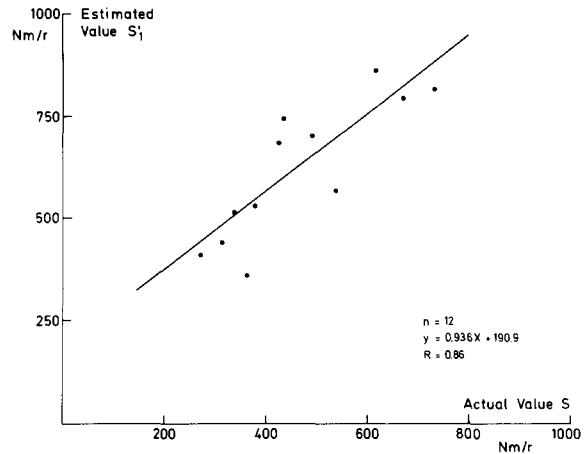


Fig. 4 a. Scatter plot for a group of femoral bone specimens correlating actual torsional stiffness versus estimated value (S_1) based upon model one, but taking into account the actual shear modulus G for each bone specimen

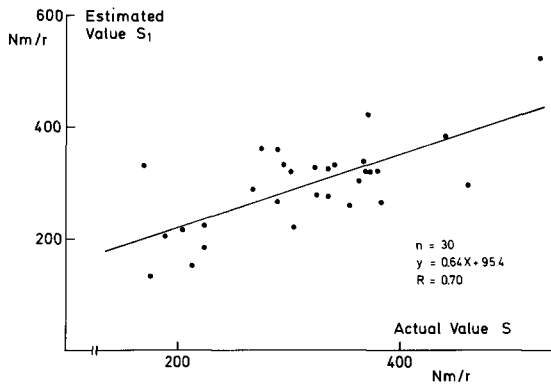


Fig. 3 b. Tibial bone specimens

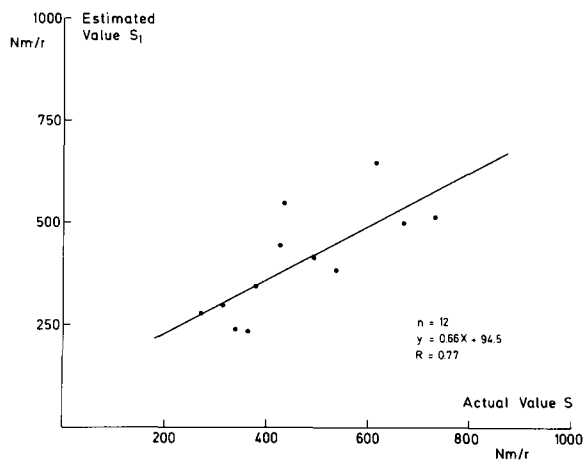


Fig. 4 b. Scatter plot for same group of femoral bone specimens but with a constant value for G for the estimated value S_1

where G_i = individual shear modulus of the mate tested for material properties.

These estimated values for torsional stiffness (S_1) are plotted versus the actual values on a scatter plot (Fig. 4 a) and for the same group of specimens a correlation was computed for the estimated value S_1 versus actual value (Fig. 4 b).

In the second model, the bone structure is assumed to have a circular ring-shaped cross section, the polar moment of which varies along the length of the bone (Fig. 7).

The torsional stiffness for each specimen can be calculated from this model using the following equation:

$$S_2 = \frac{G_m}{L} \int_0^L \frac{dz}{I_p(z)} \quad (2)$$

The nominator is calculated using the values for I_p as determined by means of the Cameron Bone Mineral Analyser, and then integrating $\frac{1}{I_p(z)}$ numerically over the length (L) of the bone.

The estimated value of torsional stiffness using this equation is correlated with the measured value for tibial and femoral bone specimens (Fig. 5).

As a check for the validity of the above described models, we also looked for the correlation between another simple mathematical model and the measured values of stiffness.

Here we assume that

$$S_1 \sim \frac{d_{\min}^4}{L}$$

where d_{\min} = minimum outer diameter of the shaft.

In the case of a circular ring cross section this would mean that the inner diameter is proportional to the outer diameter.

Ultimate Properties

Maximum torque (T_{\max}) at failure is read from the load-deformation curves for tibial and femoral bone specimens.

Maximum torque has also been calculated (T'_{\max}) using the following equation:

$$T'_{\max} = \frac{I_{p\min}}{R_{\min}} \tau_u$$

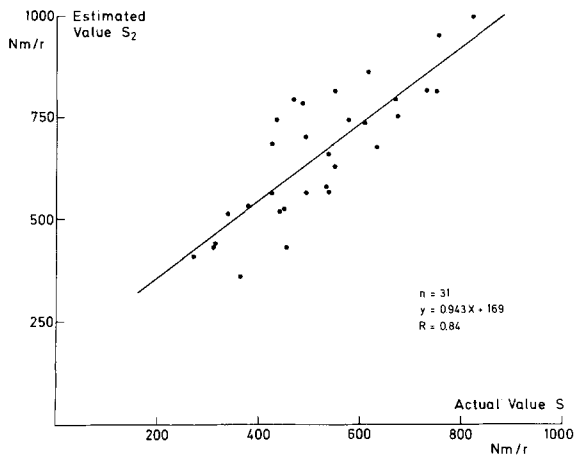


Fig. 5 a, b. Scatter plot of actual value for torsional stiffness (S) versus estimated value (S_2) assuming a ring shaped cross section with a varying polar moment of inertia along the length of the bone. **a** Femoral bone specimens

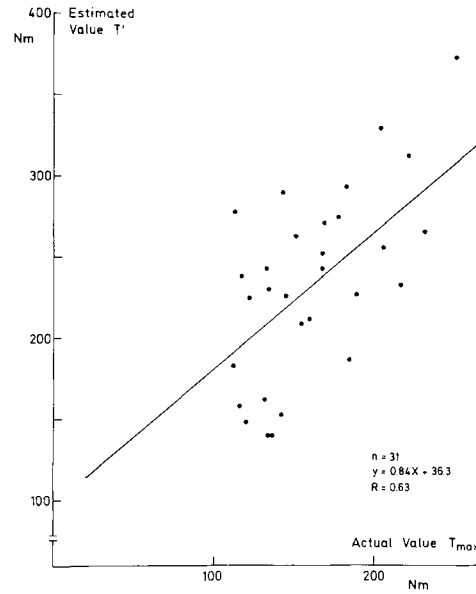


Fig. 6 a, b. Scatter plot of actual maximum torque (T_{max}) versus estimated value (T). **a** Tibial bone specimens

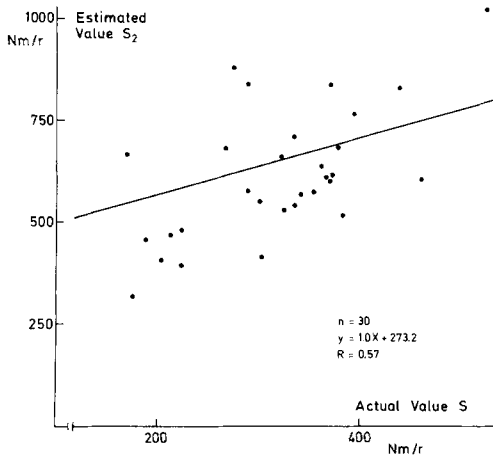


Fig. 5b. Tibial bone specimens

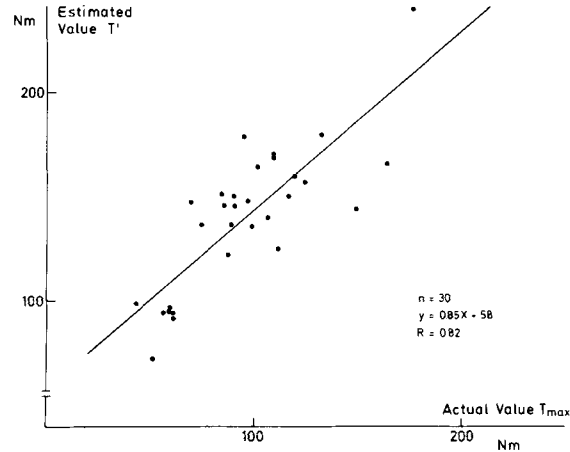


Fig. 6b. Femoral bone specimens

R_{min} = outer radius of the ring-shaped cross section of the smallest polar moment of inertia (I_{pmin}).

τ_u = the ultimate shear stress for cortical bone (= mean value of the measurements by Reilly and Burstein (1975) on twelve cylindrical samples of two human femurs (Reilly et al. 1975)).

This calculated value is correlated with the actually measured value (Fig. 6).

Since in the literature (Azang 1972) correlations have been presented between ultimate torque and some simple external dimensions of the bone as the frontal diameter of the tibial plateau, we have also looked for a correlation of T_{max} with the smallest external diameter of the bone structure (d_{min}^3) and also with the frontal diameter of the upper tibial epiphysis (D_{prox}^3).

Results and Discussion

Mechanical Properties

The mean torsional stiffness for the series ($n = 37$) of the tibial bone is 326 Nm/r and for the femoral bones ($n = 47$) 562 Nm/r. The mean maximum torque for this group of tibial bones is 101 Nm and for the femoral bone specimens 183 Nm.

The elastic (S) and ultimate properties (T_{max}) of these series of femoral and tibial bone structures show a high dispersion with a coefficient of variation for torsional stiffness (S) of 29% for femoral bones and

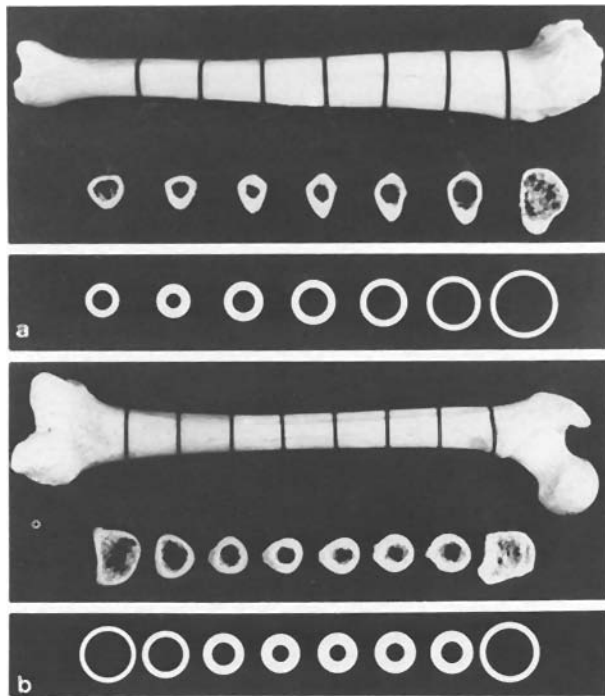


Fig. 7 a, b. The actual cross section (top) of the bone and the assumed circular ring shaped cross section (bottom) with varying polar moment along the long axis of the bone. a Femoral bone specimens. b Tibial bone specimens

31% for tibial bone specimens. The coefficient of variation for maximum torque (T_{max}) is 29% for femoral bone specimens and 34% for tibial bones.

Geometrical Properties

The plots of the polar moment of inertia (I_p) along the long axis of the bone specimen are given in Figs. 8 and 9.

Differences in geometry between the specimens are clearly visualized in these pictures. The weakest region (I_{pmin}) for the tibia is invariably located in the distal portion of the bone (Fig. 8). For the femur, however, the location of the weakest section (I_{pmin}) varies from one femoral specimens to another (Fig. 9). This explains why the fracture site in the experiments and also the clinical torsional fracture is typically situated in the distal region of the tibial bone whereas the fracture site for femoral bones varies considerably in location along the long axis of the bone.

The majority of the femoral bones presented a fracture through the proximal part of the femoral shaft and 15% of the femoral specimens revealed a fracture in the distal region of the femoral shaft. This variability in fracture location is also seen in vivo torsional fractures of the femur.

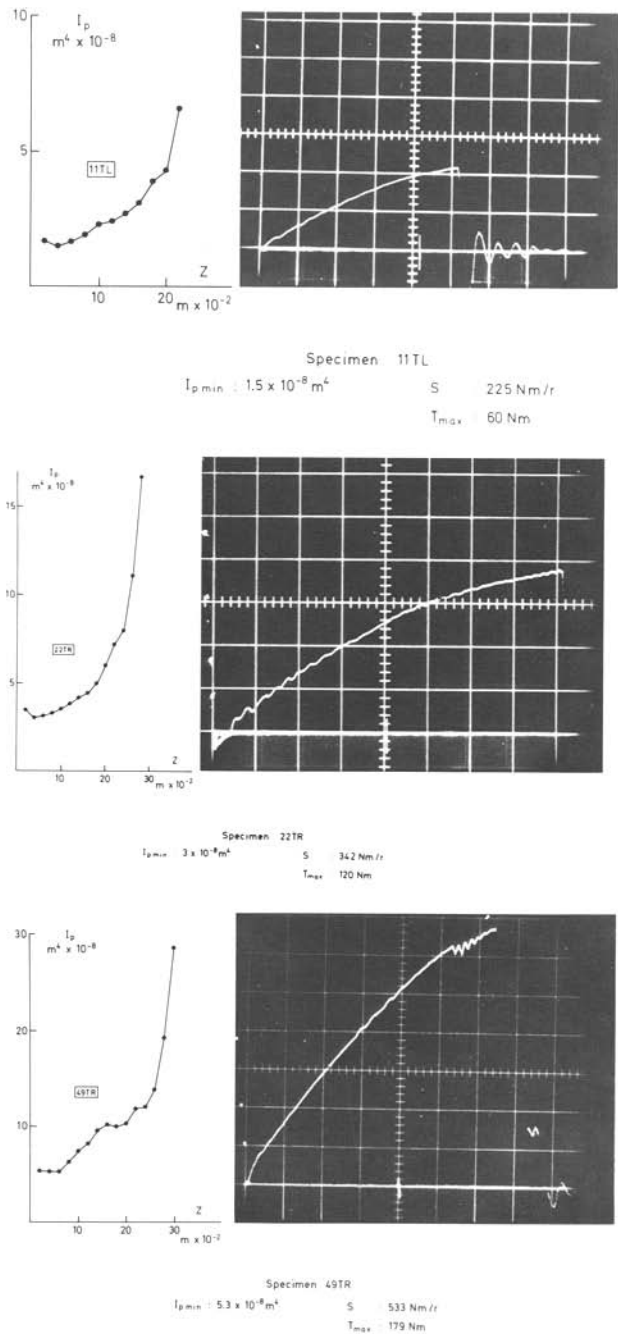


Fig. 8. Plots of the calculated polar moment of inertia (right) and load deformation curves (left) for some tibial specimens

Importance of Geometrical Properties in the Mechanical Behaviour of Bone Structures

Correlation of the estimated stiffness and maximum torque of the bone samples for the different models with the actual values allowed an evaluation of the relative importance of some geometrical and material properties to explain the high variation in mechanical behaviour of bone structures.

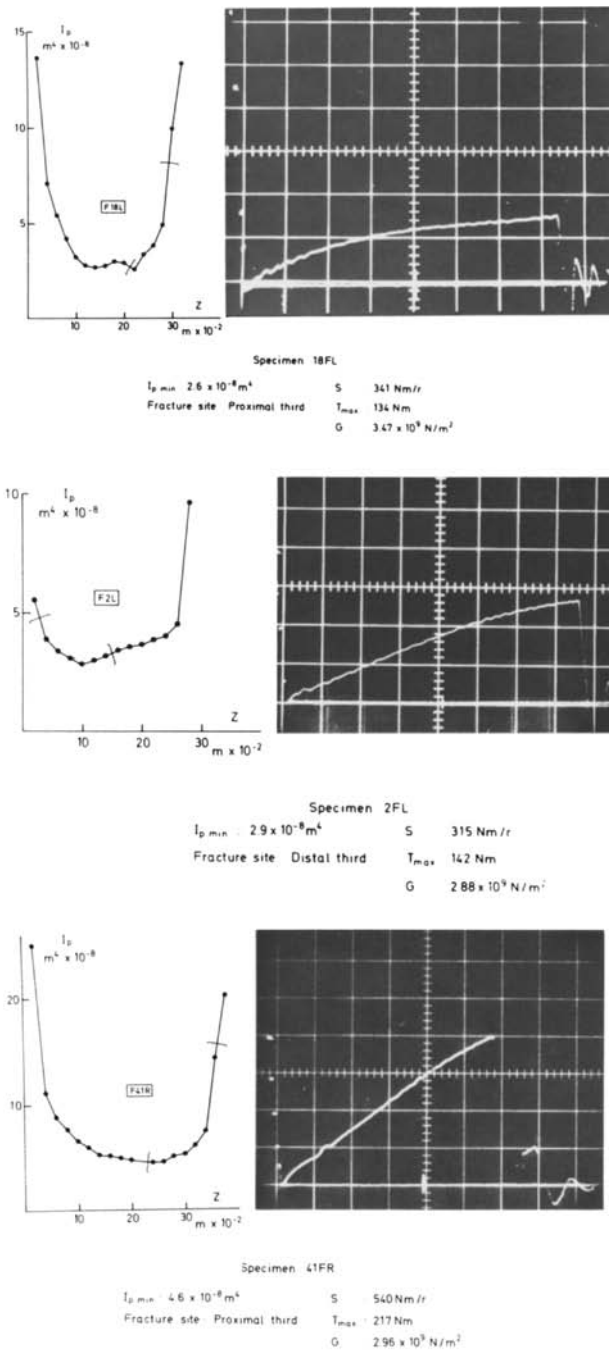


Fig. 9. Plots of the calculated polar moment of inertia (right) and load deformation curves for some femoral specimens

The accuracy of the different geometrical models is shown in the scatter plots correlating the actual values of torsional stiffness (S) or maximum torque at failure (T_{\max}) versus the estimated values using the different equations (Figs. 3–6).

Elastic Behaviour of Femoral Bone Structures in Torsional Loading

The correlation coefficient between actual and estimated torsional stiffness based upon the minimal polar moment of inertia is 0.79 which is quite high (Fig. 3). Making use of the actual material property (G) for each bone sample the correlation coefficient increases to $R = 0.84$ instead of $R = 0.77$ for the same group of bone specimens ($n = 12$) (Fig. 4).

A refinement of the geometrical model by taking into account the change of the polar moment of inertia along the long axis of the structure also improves the correlation (Fig. 5) $R = 0.84$.

These increases in R are statistically not significant. We may assume this is because of the small number of specimens.

Since a good correlation exists between the actually measured torsional stiffness and its value calculated, using a simple tube-model with $I_{p \min}$ as the polar moment of inertia, it follows that S_2 must be proportional to $I_{p \min}$. Eq (2) can be transformed to:

$$S_2 = \frac{G}{L} \int_0^L \frac{dz}{I_{pr}(z)} \cdot I_{p \min}$$

when $I_{pr}(z) = \frac{I_p(z)}{I_{p \min}}$

Hence the dispersion of $\int_0^L \frac{dz}{I_{pr}(z)}$ must be small.

The integral has been calculated for all specimens and it shows a coefficient of variation of 10% for femoral bones and 13% for tibial bone specimens.

Although the $I_{pr}(z)$ curves show important differences (Fig. 10) the area under the $1/I_{pr}(z)$ curves shows only differences of a minor degree. This indicates that it can be considered as a physical constant of the bone.

The validity of the geometrical parameter $I_{p \min}$ determined in this experimental work for the prediction of mechanical behaviour of whole bone structures in torsional loading is confirmed by the low correlation coefficients between estimated and actual values if other geometrical criteria, namely some external dimensions of bone structures, are taken into account. Correlation between actual torsional stiffness and estimated value based upon the equation

$$S \sim \frac{d_{\min}^4}{L}$$

yielded a correlation coefficient of 0.41 for the same group of femoral specimens. The difference in R is

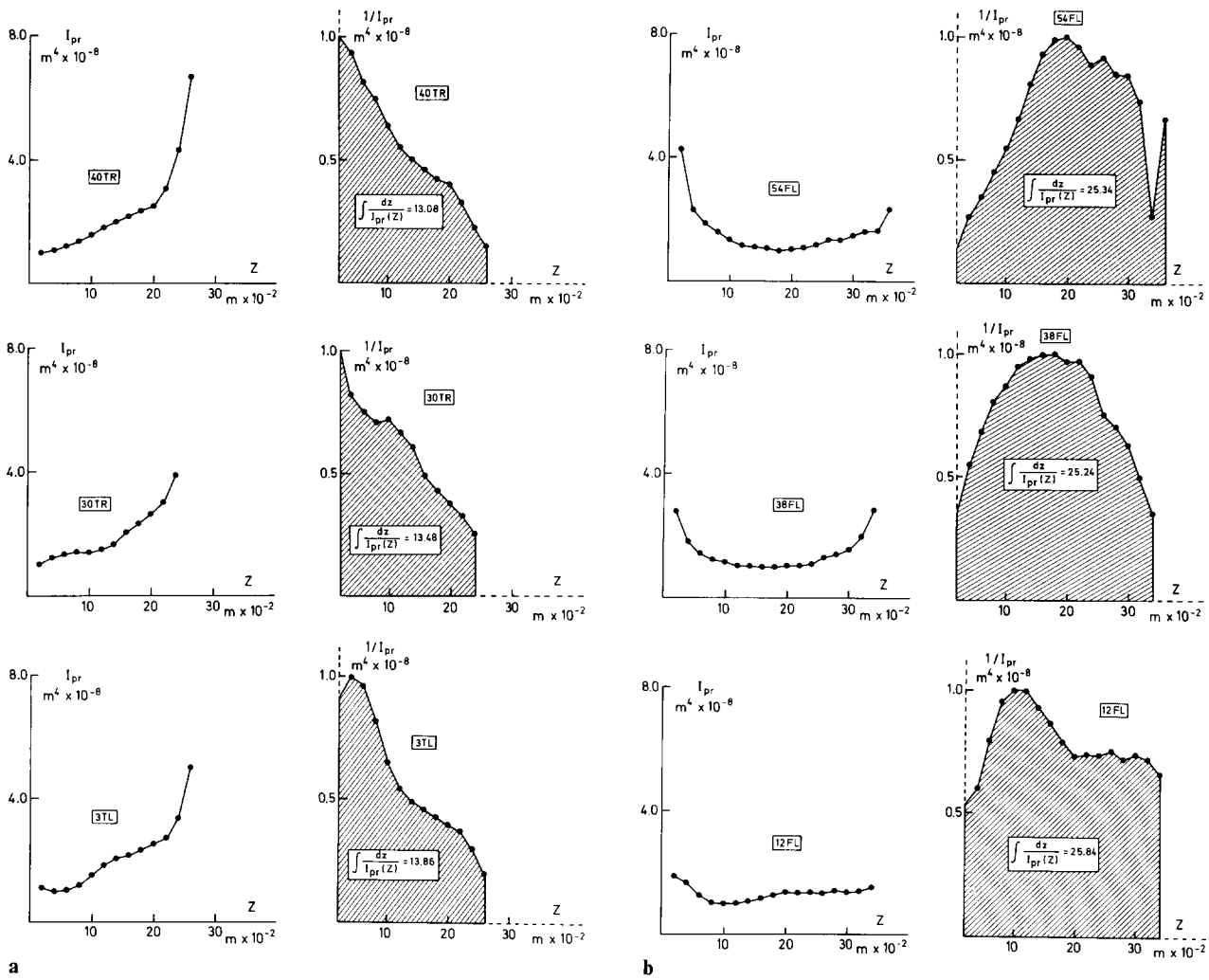


Fig. 10 a, b. On the left the $I_{pr}(z)$ curves of different specimens are shown. On the right the area under the $1/I_{pr}(z)$ curves for the same specimens. **a** Tibial bone specimens. **b** Femoral bone specimens

statistically significant ($P < 0.05$). Finally in contrast with the high correlation between geometry and elastic behaviour of femoral bone specimens a correlation could not be found for a group of twenty specimens between a material parameter (shear modulus G) and torsional stiffness (S) of the structure. $R = 0.32$. It is granted that whole bone response is a function of material properties and geometry of the structure.

However the high variation of elastic properties of femoral bone structures (c.v. 29%) is primarily dictated by the high dispersion of polar moment of inertia of the structure (c.v. 31%) where the coefficient of variation for shear modulus (G) for the same group is only 11% and the dispersion for the length of the femoral bone specimens is also relatively low (c.v. 8%). The actual load deformation curves of the specimens and resulting torsional stiffness of the structures presented in Fig. 9 illustrate how the influence of the material properties

can be ruled out by the influence of the geometry of the structure.

Tibial Bone Specimens

The correlation between estimated torsional stiffness (S) and true value is satisfactory for model one based upon the minimum polar moment of inertia $R = 0.70$.

An estimation of the elastic behaviour of tibial bone specimen based also upon the calculated variation of polar moment of inertia along the length of the specimen yields a low correlation coefficient $R = 0.57$. Although this is statistically not significantly lower than $R = 0.70$ the decrease in R for model two can be explained by the shape of the cross section area of the tibia.

This approximates only a circular ring cross section at the location of the minimum polar moment of inertia

and in contrast with femoral bone structures the cross section differ strongly from circular ring cross sections away from the zone of minimum polar moment of inertia (Fig. 7). Calculating values for I_p along the length of the tibial bones assuming circular ring cross sections yields highly incorrect values. Therefore model two estimating stiffness of a bone structure based upon polar moment of inertia of circular ring cross sections along the length a bone structure is only suitable for femur and not for tibia. Correlation between actual torsional stiffness and estimated value based upon external dimensions $S \sim \frac{d_{\min}^4}{L}$ is only 0.39.

Ultimate Properties of Bone Structures

Correlation between estimated and true value of maximum torque yields a correlation coefficient of $R = 0.63$ for femoral bone specimens and $R = 0.82$ for tibial bone specimens.

Correlation between actual ultimate torque and estimated value based upon the minimum diameter (d_{\min}^3) resulted in a $R = 0.42$ for femoral specimens and $R = 0.45$ for tibial specimens.

In contrast with Azang (1972) we could not find a definite relationship between fracture moment for torsional loading and frontal diameter of the proximal tibial epiphysis (D_{prox}). Correlation between estimated value (D_{prox}^3) and torque is 0.49.

These low values for R if other geometrical criteria are used for prediction of mechanical behaviour demonstrate that distribution of bone mass with respect to the centroid cannot be evaluated by measurement of external dimensions.

References

Azang E, Posch P, Engelbrecht R (1972) Experimentelle Untersuchungen über die Bruchfestigkeit des menschlichen Schienbeins. *Monatsschr Unfallheilk* 25:336

- Burstein AH, Currey JD, Frankel VH, Reilly DT (1972) The ultimate properties of bone tissue: The effects of yielding. *J Biomechanics* 5:35
- Burstein AH, Franekl VH (1971) A standard test for laboratory animal bone. *J Biomechanics* 4:155
- Cameron JR, Maress RB, Sorenson JA (1968) Precision and accuracy of bone mineral determination by direct photon absorptiometry. *Invest Radiol* 3:11
- Currey JD (1970) The mechanical properties of bone. *Clin Orthop* 73:210
- Ehler E, Lösche H (1970) Die menschliche Tibia unter Biegebelastung. *Beitr Orthop* 291
- Ehler E, Lösche H (1970) Biegeversuch am menschlichen Femur. *Beitr Orthop* 304
- Evans FG (1973) Mechanical properties of bone. Ch Tomas
- Frankel VH, Burstein AH (1965) Load capacity of tubular bone. In: Kenedi RM (ed) *Biomechanics and related bioengineering topics*. Pergamon Press, Oxford, p 381
- Knese KH, Hahne O, Biermann H (1956) Festigkeitsuntersuchungen an menschlichen Extremitätenknochen. *Gegenbaur Morph Jahrb* 96:141
- Martens M, Van Audekercke R, De Meester P, Mulier JC (1980) The mechanical behaviour of the long bones of the lower extremity under torsional loading. *J Biomechanics* 13:667
- Mather BS (1968) Variation with age and sex in strength of the femur. *Med Biol Engng* 6:129
- Minns RJ, Bremble GR, Campbell (1975) The geometrical properties of the human tibia. *J Biomechanics* 8:253
- Motoshima T (1960) Studies on the strength for bending of human bony extremity bones. *J Kyoto Pref Univ Med* 68:1377
- Orne D, Young DR (1976) The effects of variable mass and geometry, pretwist, shear deformation and rotatory inertia or the resonant frequencies of intact long bones: a finite element model analysis. *J Biomechanics* 9:763
- Reilly DT, Burstein AH (1974) The mechanical properties of bone. *J Bone Jt Surg* 56-A:1001
- Reilly DT, Burstein AH, Frankel V (1975) The elastic and ultimate properties of compact bone tissue. *J Biomechanics* 8:393
- Rybicki EF, Simonen FA, Weis EB (1972) On the mathematical analysis of stress in the human femur. *J Biomechanics* 5:203
- Viano D, Helfenstein V, Anlicker M, Rügsegger P (1976) Elastic properties of cortical bone in female human femurs. *J Biomechanics* 9:703

Received November 19, 1980